

Molecular g -Values, Magnetic Susceptibility Anisotropies, Molecular Quadrupole Moments and the Anisotropies in the Electronic Charge Distribution in HNO_2 -Cis, DNO_2 -Cis, HNO_2 -Trans, and DNO_2 -Trans

Dirk Hübner and Dieter H. Sutter

Abteilung Chemische Physik im Institut für Physikalische Chemie
der Christian-Albrechts-Universität Kiel

Z. Naturforsch. **39a**, 55–62 (1984); received October 12, 1983

The rotational Zeeman effect of the trans and cis forms of nitrous acid has been studied to yield the diagonal elements of the molecular g -tensor and the anisotropies in the diagonal elements of the magnetic susceptibility tensor. The results are used to calculate the diagonal elements of the molecular electric quadrupole moment tensor and the anisotropies in the second moments of the electronic charge distribution for all four molecular species. These data are compared to the corresponding CNDO/2 values, and the CNDO/2 value for the out of plane second moment of the electronic charge distribution is used together with the experimental anisotropies in the second moments of the electronic charge distribution to derive a semi-experimental value for the molecular bulk susceptibility which is otherwise difficult to obtain. The out-of-plane minus average in-plane magnetic susceptibility anisotropy is discussed with reference to the model of localised atomic susceptibilities and it is shown that the model should be extended to include bond and bond-bond interaction contributions.

Introduction

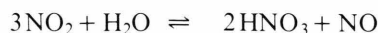
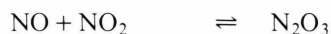
In the following we present the results of the first rotational Zeeman effect investigation of nitrous acid, a molecule known to be one of the constituents of acid rain. Such a study leads to the knowledge of the molecular g -values, of the molecular magnetic susceptibility anisotropies and of the molecular electric quadrupole moments [1–3].

The rotational spectrum of nitrous acid has been first investigated by Cox and Kuczkowski in 1966 [4] and has subsequently been extensively studied by Cox and coworkers [5, 6]. The molecule was found to exist in two planar configurations (see Fig. 1) with electric dipole moments $\mu_a = 1.378(4)\text{D}$ and $\mu_b = -1.242(15)\text{D}$ for the more abundant trans-configuration and with $\mu_a = 0.306(1)\text{D}$ and $\mu_b = 1.389(5)\text{D}$ for the cis-configuration. In both molecules the vector of the electric dipole moment closely parallels the O–H bond with oxygen at the negative and the proton at the positive end.

Experimental

The rotational Zeeman spectrograph used in this study has been described previously [7, 8]. Over-sized brass waveguide cells with inner cross sections of $1 \times 5\text{ cm}^2$ were used throughout. The Stark effect square wave modulation frequency was set to 33 kHz to reduce modulation broadening. The base line of the square wave was carefully zero based.

In the gas phase nitrous acid does not exist in pure form but is always in equilibrium with its dissociation products NO, NO_2 and H_2O which in turn are in equilibrium with N_2O_3 , N_2O_4 , HNO_3 , etc. according to reactions such as



The sample was prepared as described by Varma and Curl [9] who have studied the N_2O_3 – H_2O – HNO_2 equilibrium by intensity measurements in microwave spectroscopy. At a cell temperature of -50°C 20 mTorr of H_2O (D_2O),

Reprint requests to Prof. Dr. D. H. Sutter, Institut für Physikalische Chemie der Universität Kiel, Olshausenstr. 40, D-2300 Kiel.

0340-4811 / 84 / 0100-0055 \$ 01.3 0/0. — Please order a reprint rather than making your own copy.



Dieses Werk wurde im Jahr 2013 vom Verlag Zeitschrift für Naturforschung in Zusammenarbeit mit der Max-Planck-Gesellschaft zur Förderung der Wissenschaften e.V. digitalisiert und unter folgender Lizenz veröffentlicht: Creative Commons Namensnennung-Keine Bearbeitung 3.0 Deutschland Lizenz.

Zum 01.01.2015 ist eine Anpassung der Lizenzbedingungen (Entfall der Creative Commons Lizenzbedingung „Keine Bearbeitung“) beabsichtigt, um eine Nachnutzung auch im Rahmen zukünftiger wissenschaftlicher Nutzungsformen zu ermöglichen.

This work has been digitalized and published in 2013 by Verlag Zeitschrift für Naturforschung in cooperation with the Max Planck Society for the Advancement of Science under a Creative Commons Attribution-NoDerivs 3.0 Germany License.

On 01.01.2015 it is planned to change the License Conditions (the removal of the Creative Commons License condition “no derivative works”). This is to allow reuse in the area of future scientific usage.

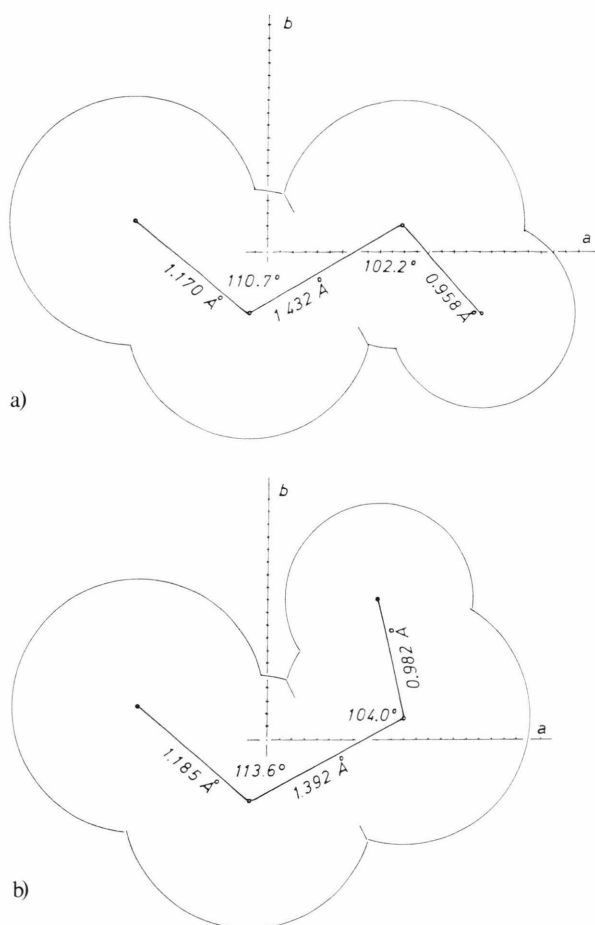


Fig. 1. R_s -structures of trans- and cis-nitrous acid as determined by Cox and coworkers [5]. These structures have been used in the further analysis of the data and as input data for the quantum chemical CNDO/2 calculation.

20 mTorr of NO and finally 40 mTorr of NO₂ were dosed into the absorption cell. Then the cell was pumped down to an overall pressure of 5 to 10 mTorr and the measurements were started immediately since the sample proved to be unstable in our absorption cells. The decay of the absorption signal due to undefined wall reactions, not included in the reaction equations mentioned above, had a half time of about 10 min. Thus several subsequent fillings and signal averaging had to be used to record the weaker transitions. In Fig. 2 we present a section of the Zeeman hyperfine pattern of the 4 0 4 → 3 1 3 rotational transition of trans-DONO in order to give an impression of the resolution and signal to noise ratio which was achieved in the

present investigation for the more abundant trans-species. A complete listing of the observed Zeeman hyperfine splittings may be obtained upon request from the authors.

Analysis of the Data

The analysis of the Zeeman-hyperfine splittings was based on the effective rotational Hamiltonian given in (1), [10], and [11]:

$$\hat{H}_{\text{eff}} = \hat{H}_{\text{RR}} + \hat{H}_{g_1(^{14}\text{N})} + \hat{H}_{Q(^{14}\text{N})} + \hat{H}_g + \hat{H}_x. \quad (1)$$

In Eq. (1), the operators at the right hand side correspond to the rigid rotor Hamiltonian \hat{H}_{RR} , the ¹⁴N nuclear quadrupole coupling Hamiltonian, $\hat{H}_{Q(^{14}\text{N})}$, the first and second order molecular rotational Zeeman effect Hamiltonians \hat{H}_g and \hat{H}_x , and the ¹⁴N nuclear Zeeman effect Hamiltonian, $\hat{H}_{g_1(^{14}\text{N})}$.

Deuterium quadrupole hyperfine interaction, spin rotation coupling and the nuclear Zeeman effect Hamiltonians of the nuclei other than ¹⁴N were neglected. (To an excellent approximation the other nuclei may be regarded as cardanically suspended within the molecule with their spins processing freely about the magnetic field axis.)

As described in detail in [11], the Hamiltonian matrix corresponding to (1) was set up in the uncoupled basis $|J, K_-K_+, M_J, I(^{14}\text{N}), M_I(^{14}\text{N})\rangle$. Matricelements which connect different rotational states $J, K_-K_+ \leftrightarrow J', K'_-K'_+$, and which arise from $\hat{H}_{Q(^{14}\text{N})}$, \hat{H}_g , and \hat{H}_x , were neglected, since their second order contributions to the rotational levels may be estimated to be well below the resolution power of the spectrograph.

The resulting $M_J, M_I(^{14}\text{N})$ -submatrices corresponding to the individual rotational states J, K_-K_+ were diagonalized numerically [12]. The corresponding unitary transformations were used to calculate relative intensities of the individual satellites. The diagonal elements of the molecular g -tensors and the anisotropies in the diagonal elements of the molecular magnetic susceptibility tensors which result from a least squares fit to the observed splittings are given in Table 1. Also given are our ¹⁴N quadrupole coupling constants which were fitted to the zero field hyperfine splittings. Within the standard deviations of the fit they agree with those reported earlier by Cox and coworkers. In Table 2 we give the rotational constants and the atom coordinates with respect to the principal

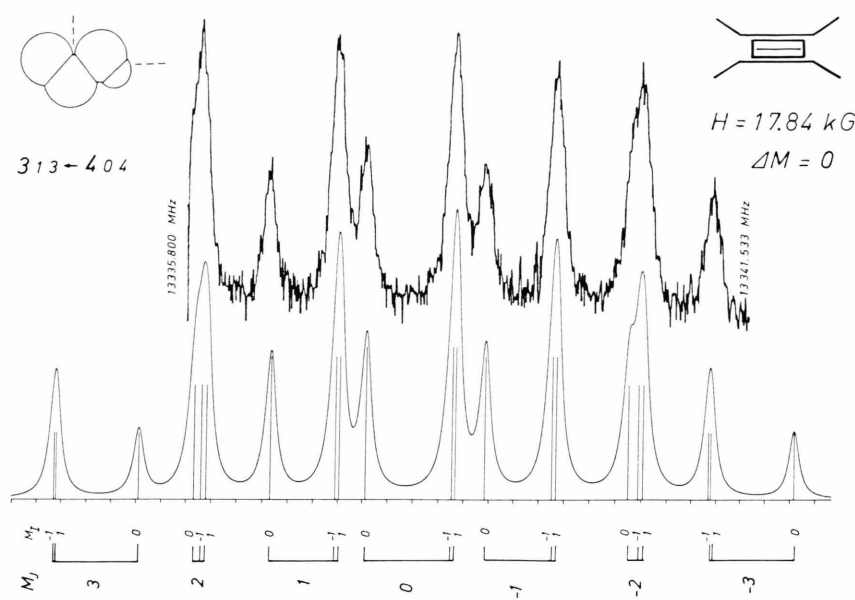


Fig. 2. Section of the $3_{13} \leftarrow 4_{04}$ rotational transition of trans deuterio nitrous acid observed under $\Delta M = 0$ selection rule. ^{14}N quadrupole coupling causes each $M_j \leftarrow M_j'$ satellite to split into a triplet corresponding to $M_I = \pm 1$ and $M_I = 0$.

molecular g -values	g_{aa}	-0.9452 (12)	-0.7869 (17)	-1.2373 (6)	-1.2101 (6)
$g_{aa} = \frac{m_p}{I_{aa}} \left[\sum_n^{nuclear} Z_n (b_n^2 + c_n^2) + \frac{2}{m} \left(\frac{L_a L_a}{\Delta} \right) \right]$	g_{bb}	-0.1390 (5)	-0.1367 (12)	-0.1065 (3)	-0.0977 (3)
	g_{cc}	-0.0542 (6)	-0.0520 (11)	-0.0425 (3)	-0.0397 (3)
magnetic susceptibility anisotropies (10^{-6} erg G $^{-2}$ mole $^{-1}$)	$2\chi_{aa} - \chi_{bb} - \chi_{cc}$	21.3 (11)	21.0 (13)	25.5 (6)	25.7 (5)
$\chi_{aa} = -N \frac{e^2}{2m_c^2} \left[\left(\sum_n^{nuclear} b_n^2 + c_n^2 \right) + \frac{2}{m} \left(\frac{L_a L_a}{\Delta} \right) \right]$	$2\chi_{bb} - \chi_{cc} - \chi_{aa}$	7.4 (8)	10.4 (10)	4.0 (5)	2.0 (4)
$\left(\frac{L_a L_a}{\Delta} \right) = \frac{\sum_n^{exc} \langle n L_a 0 \rangle \langle 0 L_a n \rangle}{E_0 - E_n}$					
^{14}N nuclear quadrupole coupling constants (MHz)	$^{14}\chi_{bb} + ^{14}\chi_{cc}$	-2.111 (35)	-2.191 (32)	-1.839 (26)	-1.747 (20)
	$^{14}\chi_{bb} - ^{14}\chi_{cc}$	-9.609 (78)	-9.688 (71)	-8.881 (69)	-8.809 (49)

Table 1. Diagonal elements of the molecular g -tensor, molecular susceptibilities and ^{14}N nuclear quadrupole coupling constants determined in this work. Only the relative sign of the g -values is determined by the experiment. In nitrous acid the sign is however uniquely determined from the nuclear contribution to g_{aa} , from the fact that the perturbation sum is necessarily negative and from the absolute value of g_{aa} . (Compare the theoretical expression for g_{aa} given in the Table.)

rotational constants	A/MHz	84101.72(59)	70815.25(39)	92889.06(6)	89364.60(6)
$A = \frac{h}{8 \pi^2 I_{aa}}$ etc.	B/MHz	13168.99(9)	12899.16(7)	12524.75(3)	11667.28(3)
	C/MHz	11364.25(8)	10891.24(6)	11016.82(3)	10303.90(3)
r_s - coordinates in Å units	$a_{(Oz)}$	- 1.038	- 1.050	- 1.061	- 1.102
	$a_{(-Nx)}$	- 0.140	- 0.174	- 0.153	- 0.178
	$a_{(-O-y)}$	1.105	1.089	1.085	1.044
	$a_{(H-)}, a_{(D-)}$	0.890	0.903	1.730	1.704
	$b_{(Oz)}$	0.248	0.257	0.242	0.227
	$b_{(-Nx)}$	- 0.501	- 0.519	- 0.496	- 0.490
	$b_{(-O-y)}$	0.123	0.067	0.224	0.257
	$b_{(H-)}, b_{(D-)}$	1.081	1.032	- 0.485	- 0.437

Table 2. Rotational constants and r_s -coordinates [5] used in the further analysis of the Zeeman data.

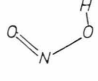
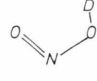
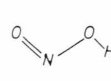
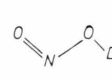
					
molecular quadrupole moments / (10 ⁻²⁶ esu cm ²)	Q_{aa}	-3.43(77)	-3.57(103)	2.78(42)	3.36(37)
$Q_{aa} = \frac{ieI}{2} \left[\sum_n^{nuc[ei]} \{ 2a_n^2 - b_n^2 - c_n^2 \} - \langle \sum_n^{electr} 2a_e^2 - b_e^2 - c_e^2 \rangle \right]$ $= -\frac{h eI }{16\pi^2 m} \left\{ \frac{2g_{aa}}{A} - \frac{g_{bb}}{B} - \frac{g_{cc}}{C} \right\}$ $- \frac{2\pi I c^2}{ieI N_L} \{ 2\chi_{aa} - \chi_{bb} - \chi_{cc} \}$	Q_{bb}	1.96(63)	0.51(94)	-2.47(38)	-1.91(33)
	Q_{cc}	1.47(127)	3.06(169)	-0.31(72)	-1.45(62)
paramagnetic susceptibilities / (10 ⁻⁶ erg G ⁻² mole ⁻¹)	χ_{aa}^p	38.96(7)	38.56(9)	40.37(6)	40.80(6)
$\chi_{aa}^p = N_L \frac{e^2}{2m^2 c^2} \left(-\frac{L_a L_a}{\Delta} \right)$ $= \frac{e^2 N_L}{2m c^2} \left\{ \frac{h}{16\pi^2 m_p} - \frac{g_{aa}}{A} - \frac{1}{2} \sum_n^{nuc[ei]} Z_n (b_n^2 + c_n^2) \right\}$	χ_{bb}^p	104.47(12)	104.56(24)	109.70(9)	109.34(10)
	χ_{cc}^p	107.18(15)	107.06(26)	111.81(10)	111.68(10)
second moments of the electronic charge distribution / Å ²	$\langle \sum a_e^2 - b_e^2 \rangle$	16.53(20)	16.38(26)	18.02(12)	18.01(11)
$\langle \sum a_e^2 - b_e^2 \rangle = \sum_n^{nuc[ei]} Z_n (a_n^2 - b_n^2)$ $+ \frac{h}{8\pi^2 m_p} \left\{ \frac{g_{aa}}{A} - \frac{g_{bb}}{B} \right\} + \frac{4m c^2}{e^2 N_L} \{ \chi_{aa} - \chi_{bb} \}$	$\langle \sum b_e^2 - c_e^2 \rangle$	3.47(27)	3.86(37)	3.13(16)	2.88(14)
	$\langle \sum c_e^2 - a_e^2 \rangle$	-20.00(28)	-20.24(36)	-21.15(16)	-20.89(14)

Table 3. Molecular electric quadrupole moments, paramagnetic susceptibilities and anisotropies in the second moments of the electronic charge distribution. These data can be derived from the experimental values, listed in Tables 1 and 2. For the effects of vibrational averaging, the reader is referred to [3].

inertia axes systems. The latter are calculated from the r_s -structures determined to Cox et al. [5]. In Table 3 we give the molecular electric quadrupole moments, the paramagnetic susceptibilities and the anisotropies in the second moments of the electronic charge distribution, which can be derived from the observed g -values and susceptibility anisotropies by use of their theoretical expressions [13, 14]. Together with the knowledge of the electric dipole moments, the knowledge of the electric quadrupole moments is of prime interest for the understanding of rotational relaxation channels [15].

Discussion

It is interesting to compare the experimentally determined molecular quadrupole moments and anisotropies in the second moments of the electronic charge distribution with the corresponding values calculated from CNDO/2 wavefunctions as described in [16]. The latter are presented in Table 4. In most cases the values agree within two standard deviations of the experimental data. This encourages us to use the CNDO/2 out of plane second moments of the electronic charge distribu-

tion $\left\langle 0 \left| \sum_e^{\text{electrons}} c_e^2 \right| 0 \right\rangle$, together with the experimental anisotropies in the second moments of the electronic charge distribution to predict all three second moments together with the individual components of the diamagnetic susceptibility tensor.

In this way the values in Table 5 are obtained. Furthermore if we make use of our experimental knowledge of the paramagnetic susceptibilities, we are also in the position to derive values for the individual components of the magnetic susceptibility tensor and of the bulk susceptibilities, values, which are not easily accessible otherwise. They too are listed in Table 5.

We now turn to the model of local atom susceptibilities [18]. We restrict our discussion to the out of plane minus average in plane anisotropy, $\chi_{\perp} - \chi_{\parallel} = \chi_{cc} - (\chi_{aa} + \chi_{bb})/2$, a quantity which is directly determined in the rotational Zeeman effect experiment and which is of prime interest in the discussion of ring currents in aromatic molecules.

We first note that in accordance with the model of local susceptibilities all four species studied in this investigation have, essentially within the

$Q_{aa} / 10^{-26} \text{esu cm}^2$	-4.299	-4.104	0.848	0.891
$Q_{bb} / 10^{-26} \text{esu cm}^2$	2.190	1.960	-1.737	-1.843
$Q_{cc} / 10^{-26} \text{esu cm}^2$	2.109	2.144	0.889	0.951
$\langle \sum a_e^2 \rangle / 10^{-16} \text{ cm}^2$	22.943	22.927	24.324	24.310
$\langle \sum b_e^2 \rangle / 10^{-16} \text{ cm}^2$	6.265	6.277	5.933	5.942
$\langle \sum c_e^2 \rangle / 10^{-16} \text{ cm}^2$	2.737	2.737	2.742	2.742
$\langle \sum a_e^2 - b_e^2 \rangle / 10^{-16} \text{ cm}^2$	16.677	16.650	18.391	18.368
$\langle \sum b_e^2 - c_e^2 \rangle / 10^{-16} \text{ cm}^2$	3.528	3.539	3.191	3.200
$\langle \sum c_e^2 - a_e^2 \rangle / 10^{-16} \text{ cm}^2$	-20.205	-20.189	-21.582	-21.568
$\chi_{aa}^d / 10^{-6} \text{erg G}^{-2} \text{mole}^{-1}$	-38.19	-38.24	-36.80	-36.84
$\chi_{bb}^d / 10^{-6} \text{erg G}^{-2} \text{mole}^{-1}$	-108.95	-108.88	-114.83	-114.77
$\chi_{cc}^d / 10^{-6} \text{erg G}^{-2} \text{mole}^{-1}$	-123.92	-123.90	-128.37	-128.35

Table 4. Molecular quadrupole moments, second moments of the electronic charge distribution and diamagnetic susceptibilities calculated from CNDO/2 wave functions. Equation (18) of [16] and the r_s -coordinates given in Table 2 were used in this calculation. Our program is based on the original parametrization of Pople et al.

$\langle \sum c_e^2 \rangle_{\text{CNDO}/2}$	2.74 (20)	2.74 (20)	2.74 (20)	2.74 (20)
$\langle \sum a_e^2 \rangle^*$	22.74 (34)	22.98 (40)	23.89 (26)	23.63 (24)
$\langle \sum b_e^2 \rangle^*$	6.21 (34)	6.60 (41)	5.87 (26)	5.62 (24)
$\chi_{aa}^{d*} = -\frac{N_L e^2}{4m c^2} [\langle \sum b_e^2 \rangle^* \cdot \langle \sum c_e^2 \rangle_{\text{CNDO}}]$	-38.0 (17)	-39.6 (19)	-36.5 (14)	-35.5 (13)
$\chi_{bb}^{d*} = -\frac{N_L e^2}{4m c^2} [\langle \sum c_e^2 \rangle_{\text{CNDO}} \cdot \langle \sum a_e^2 \rangle^*]$	-108.1 (17)	-109.1 (19)	-113.0 (14)	-111.9 (13)
$\chi_{cc}^{d*} = -\frac{N_L e^2}{4m c^2} [\langle \sum a_e^2 \rangle^* \cdot \langle \sum b_e^2 \rangle^*]$	-122.8 (17)	-125.5 (24)	-126.3 (16)	-124.1 (14)
χ_{aa}^*	1.0 (17)	-1.1 (19)	3.8 (14)	5.3 (13)
χ_{bb}^*	-3.6 (17)	-4.6 (19)	-3.3 (14)	-2.5 (13)
χ_{cc}^*	-15.7 (17)	-18.4 (24)	-14.5 (16)	-12.4 (24)
$\chi_{cc \text{ average}}$		-15.3 (26)		
$\chi_{\text{bulk average}}$		-5.5 (23)		

Table 5. For comparison of Tables 3 and 4 we conclude that the CNDO/2-value for $\langle 0 | \sum_e c_e^2 | 0 \rangle$ is correct within $\pm 0.2 \text{ \AA}^2$, and we use it together with the experimental

values for the anisotropies of the second moments of the electronic charge distribution to calculate the semiexperimental values for the diamagnetic susceptibilities.

Together with the paramagnetic susceptibilities these values lead to semiexperimental values for the diagonal elements of the susceptibility tensor.

Even within an extended additivity scheme which includes bond and bond-bond interaction contributions χ_{\perp} and χ_{bulk} should be the same for all four molecules. We therefore present their average as most probable values.

The asterisk is used to remind the reader to the semiexperimental nature of the data. Quoted uncertainties result from the experimental uncertainties in the input data and a 0.2 \AA uncertainty in the $\langle \sum_e c_e^2 \rangle$ value.

experimental uncertainties, the same out of plane minus average in plane value i.e.

$$(\chi_{\perp} - \chi_{\parallel}) = -(14.7 \pm 0.6) \cdot 10^{-6} \text{ erg G}^{-2} \text{ mol}^{-1}.$$

But if we use this value together with the “known” anisotropies for Hydrogen and Oxygen

$$(\chi_{\perp} - \chi_{\parallel})_{(\text{H-})} = -0.41 \cdot 10^{-6} \text{ erg G}^{-2} \text{ mol}^{-1},$$

$$(\chi_{\perp} - \chi_{\parallel})_{(\text{O-})} = +1.23 \cdot 10^{-6} \text{ erg G}^{-2} \text{ mol}^{-1},$$

and

$$(\chi_{\perp} - \chi_{\parallel})_{(\text{O=})} = -6.01 \cdot 10^{-6} \text{ erg G}^{-2} \text{ mol}^{-1};$$

(see Table 6 in [19]) to derive the contribution of

the Nitrogen atom, we arrive at

$$(\chi_{\perp} - \chi_{\parallel})_{(\text{N=})} = -9.51 \cdot 10^{-6} \text{ erg G}^{-2} \text{ mol}^{-1},$$

a value which deviates considerably from the value of

$$(\chi_{\perp} - \chi_{\parallel})_{(\text{N=})} = -4 \cdot 10^{-6} \text{ erg G}^{-2} \text{ mol}^{-1}$$

proposed earlier by Rohwer, Guarnieri, and Wiese on the basis of the Zeeman data obtained for $\text{O}=\text{N}-\text{F}$ [20]. (The observed difference could be due to a rather important contribution from ionic structures in Nitrosyl Fluoride, which were suggested earlier by Buckton, Legon, and Millen [24] from the structure and from the quadrupole

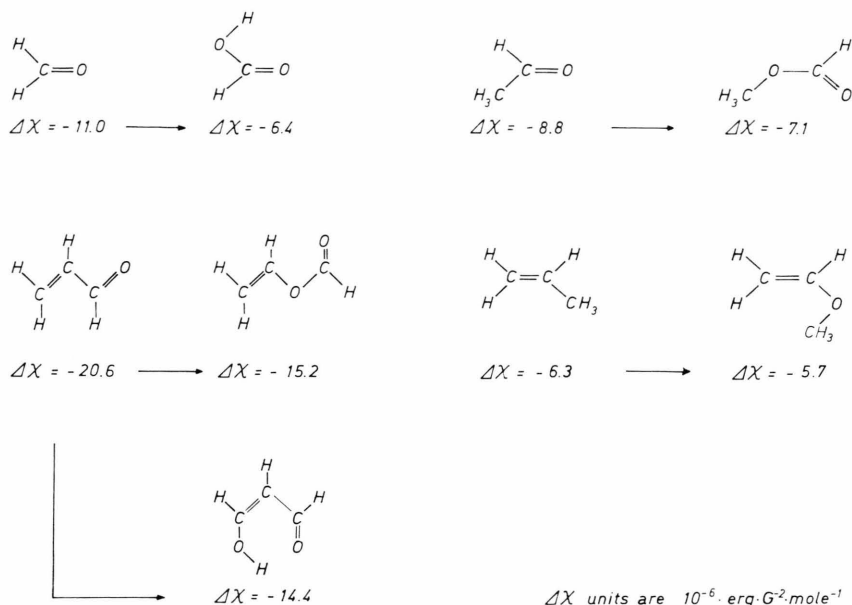


Fig. 3. The simple additivity scheme of local atom susceptibility tensors also runs into problems, when oxygen is inserted into single bonds. If the scheme were valid $\Delta\chi = \chi_{\perp} - \chi_{\parallel}$ should change (within the experimental uncertainties) by the same amount in all five cases, but we can clearly distinguish a group in which the change is about +5.5 units (left) and a group in which the change is about +1 unit (right). Such observations indicate that the additivity scheme has to be extended to include bond and bond-bond interaction contributions similar to the procedure proposed by Hameka [21] for the bulk susceptibilities.

coupling constants in Nitrosyl Chloride. This of course makes Nitrosyl Fluoride the poorer candidate to determine $(\chi_{\perp} - \chi_{\parallel})$ for pyridinic nitrogen, but also demonstrates the importance of the bonding situation for the locally induced magnetic moments.)

Similar problems with the simple additivity scheme of local atomic susceptibility tensors arise in several cases where single bonds are replaced by an oxygen-bridge as is shown in Figure 3. Within the simple additivity scheme, oxygen insertion should change $(\chi_{\perp} - \chi_{\parallel})$ essentially by the same amount in all molecules but it is obvious that there is only a small change (i.e. about +1 unit), when $-\text{O}-$ is inserted into a $\text{C}-\text{CH}_3$ bond, but that there is a rather large change (i.e. five to six units) when oxygen is inserted into a $\text{C}-\text{H}$ bond. These examples clearly demonstrate that the simple model must be extended to include contributions of the bonds and of bond-bond-interactions similar to the method proposed and developed by Hameka and coworkers [21] for the calculation of bulk susceptibilities. To provide the experimental basis for

such an extension further rotational Zeeman effect studies are essential.

Finally we briefly discuss the observed quadrupole moments.

In principle the molecular electric quadrupole moments may be used to detect changes in the electronic configuration. Thus, if for instance the change from the cis- to the trans-configuration left the internal electronic configurations of the $\text{O}=\text{N}$ -frame and of the $\text{O}-\text{H}$ -top unchanged and simply consisted in a 180° rotation of the latter around the $\text{N}-\text{O}$ -bond, the out of plane quadrupole moments should be related as

$$\begin{aligned}
 (Q_{cc}^{\text{cis}} - Q_{cc}^{\text{trans}}) \\
 = -[a_0(\mu_a^{\text{cis}} - \mu_a^{\text{trans}}) + b_0(\mu_b^{\text{cis}} - \mu_b^{\text{trans}})],
 \end{aligned}$$

where a_0 , b_0 are the coordinates of any point on the axis of internal rotation. For convenience we choose the average coordinates of the Oxygen atom. With this choice and the experimental values for the quadrupole moments and electrical dipole moments

we would predict within this model

$$\begin{aligned}(Q_{cc}^{\text{cis}} - Q_{cc}^{\text{trans}})_{\text{pred}} &= -[1.06 \cdot (0.306 - 1.378) \\ &\quad - 0.24 \cdot (1.389 + 1.242)] \\ &\quad \cdot 10^{-26} \text{ esu cm}^2 \\ &= 1.77 \cdot 10^{-26} \text{ esu cm}^2\end{aligned}$$

as compared to the experimentally observed difference:

$$\begin{aligned}(Q_{cc}^{\text{cis}} - Q_{cc}^{\text{trans}})_{\text{exp}} &= 1.78 (145) \cdot 10^{-26} \text{ esu cm}^2 \\ &\quad \text{for the normal species ,} \\ &= 4.51 (221) \cdot 10^{-26} \text{ esu cm}^2 \\ &\quad \text{for the deuterated species .}\end{aligned}$$

Although the observed difference can be roughly predicted with the simple model, the experimental

accuracy has to be improved before molecular quadrupole moments determined from rotational Zeeman effect studies can be used for a critical discussion of electronic structure. However, if it should prove possible to use microwave Fourier transform spectroscopy [22, 23] also for rotational Zeeman effect studies, the higher resolution necessary for such discussions may soon become available.

We gratefully acknowledge the financial support by Deutsche Forschungsgemeinschaft and Fonds der Chemischen Industrie. We thank Prof. A. Guarnieri for critically reading the manuscript. All computer calculations were carried out at the computer center of the Christian-Albrechts-University at Kiel.

- [1] W. H. Flygare and R. C. Benson, *Mol. Phys.* **20**, 225 (1971).
- [2] W. H. Flygare, *Chem. Rev.* **74**, 653 (1973).
- [3] D. H. Sutter and W. H. Flygare, *Topics in Current Chem.* **63**, 89 (1976).
- [4] A. P. Cox and R. L. Kuczkowski, *J. Amer. Chem. Soc.* **88**, 5071 (1966).
- [5] A. P. Cox, A. H. Brittain, and D. J. Finnigan, *Trans. Faraday Soc.* **67**, 2179 (1971).
- [6] D. J. Finnigan, A. P. Cox, A. H. Brittain, and J. G. Smith, *J. Chem. Soc. Faraday Trans. II*, **68**, 548 (1972).
- [7] D. H. Sutter, *Z. Naturforsch.* **26a**, 1644 (1971).
- [8] Ref. [3], Chapt. III A.
- [9] Ravi Carma and R. F. Curl, *J. Phys. Chem.* **80**, 402 (1976).
- [10] Ref. [3], Chapt. III E.
- [11] K. F. Dössel, J. Wiese, and D. H. Sutter, *Z. Naturforsch.* **33a**, 21 (1978).
- [12] The computer routine DZQDG. F4 developed by E. Hamer (E. Hamer, Thesis, University Kiel, 1973) was used.
- [13] J. R. Eshbach and M. W. P. Strandberg, *Phys. Rev.* **85**, 24 (1952).
- [14] J. H. van Vleck, *The Theory of Electric and Magnetic Susceptibilities*. Oxford University Press, London 1936.
- [15] T. Oka, *Adv. At. Mol. Phys.* **9**, 127 (1973).
- [16] Eilert Hamer, Dissertation, Universität Kiel (1973). Chap. II.1.
- [17] E. Hamer, L. Engelbrecht, and D. H. Sutter, *Z. Naturforsch.* **29a**, 924 (1974), Eq. (18).
- [18] R. C. Benson and W. H. Flygare, *J. Amer. Chem. Soc.* **92**, 7523 (1970).
- [19] J. Wiese and D. H. Sutter, *Z. Naturforsch.* **35a**, 712 (1980).
- [20] F. Rohwer and A. Guarnieri, *Z. Naturforsch.* **35a**, 336 (1980).
- [21] P. S. O'Sullivan and H. F. Hameka, *J. Amer. Chem. Soc.* **91**, 25 (1970).
- [22] G. Bestmann, H. Dreizler, H. Mäder, and U. Andresen, *Z. Naturforsch.* **35a**, 392 (1980).
- [23] G. Bestmann and H. Dreizler, *Z. Naturforsch.* **37a**, 58 (1982).
- [24] K. S. Buckton, A. C. Legon, and D. J. Millen, *Trans. Faraday Soc.* **65**, 1975 (1969).